rf2022.com

Home | Important Dates | Registration | Program | Video Clip Contest | Paper Submission | more...

THE 20th ANNIVERSARY EDITION OF RIVER FLOW CONFERENCES !

****** Important Updates ******

1. Owing to various requests, we will keep registration open until Wednesday, November 9, at 5pm (Toronto time).
However, at this point access to the conference will only be given starting on the day after registration.
That is, anyone registering on November 8, will get access to the conference on Nov 9 and 10.
Anyone registering on November 9, will get access to the conference on Nov 10.

RIVER FLOW 2022 - Full Program

Toronto time = EST (Eastern Standard Time); Coleman Award submissions marked with (**)

Tuesday – November 8th, Morning

08:15	Opening Ceremony				
08:45	**Keynote Lecture 1** **Unveiling the diversity of river systems in Lowland Amazonia: from basic science to engineering projects to achieve sustainable river-based development** ***Dr. Jorge D. Abad, Scientific Director, RED YAKU, Peru***				
09:45	Morning Break				
10:15	Parallel Sessions 1				
	A1: Flow in Straight and Compound Channels – Part I ***Chair: Donatella Termini*** ***University of Palermo, Italy***	**A2: Coherent Structures in Open-Channel Flow** ***Chair: Vincent Chu*** ***McGill University, Canada***	**C1: In-Stream Structures: Hydrodynamics, Scour and Riverbed Protection – Part I** ***Chair: Rob Ettema*** ***Colorado State University, USA***	**D1: Flow in Vegetated Channels** ***Chair: Jay Lacey*** ***Université Sherbrooke, Canada***	**E1: Contaminant Transport and Mixing Processes – Part I** ***Chair: Susan Gaskin*** ***McGill University, Canada***
10:20	Apparent shear force modelling in compound open channel using Support Vector Machine (**) ***P. Gaurav, B. Das, J. Khuntia, V. Devi***	Large-scale motion over spanwise heterogeneous bed roughness ***S. Chung, Q. Luo, T. Stoesser***	Discussion of various equilibrium concepts on scouring around hydraulic structures (**) ***C. Kannen, F. Seidel, M. Franca***	Effects of patch height on sediment entrainment mechanisms around a rectangular patch of vegetation ***M. Koken, G. Constantinescu***	Gravity currents flowing over a rough bed (**) ***M. Maggi, C. Adduce, M. Negretti***
10:40	Flow structure in a compound channel flow: benchmarking 2D and 3D numerical models ***I. Kimura, D. Bousmar et al.*** ***IAHR Working Group on Compound Channels***	Three-dimensional structures of ice-covered flow in a river bend: ***T. Ge, B. Koyuncu***	Surface bed characteristics of circular pier scouring in different sediment mixtures under flow shallowness variations (**) ***S. Okhravi, Y. Velísková, S. Gohari, T. Fazeres-Ferradosa,***	Direct bed shear stress measurements in flows through rigid emergent vegetation (**) ***J. Aliaga, J. Aberle***	Influence of an emergent vertical obstacle on approaching gravity current (**) ***G. Di Lollo, C. Adduce, M. Brito, R. Ferreira, A. Ricardo***
11:00	Boundary shear stress induced by a ship propeller wake over rough and smooth bed surfaces ***F. Núñez, J. Macías, J. Aberle***	Cylindrical obstacle impacted by long waves: experimental observation of downstream vorticity and coherent structures ***F. De Serio, R. Basile***	Riverbed protection due to installation of stacked boulders on both sides of elliptical pier ***T. Ishitsuka, Y. Yasuda***	Anisotropy in turbulent flow through random and emergent rigid vegetation on rough beds ***N. Penna, F. Coscarella, R. Gaudio, P. Gualtieri***	Quantifying mixing processes at a river-lake interface: the case of the plunging negatively buoyant inflow of the Rhône R. into Lake Gen. (**) ***S. Thorez, K. Blanckaert, U. Lemmin, D. Barry***
11:20	A Rational estimation of the fully developed approach flow required for fluid-structure interaction studies in an open channel ***S. Das, R. Balachandar, R. Barron***	Large-scale motion in semi-filled pipes and very narrow channels at supercritical flow ***Y. Liu, T. Stoesser***	The impact of river ice submergence and length on local scour (**) ***D. Sirianni, C. Valela, C. Rennie, I. Nistor, H. Almansour***	Direct visualization of hyporheic exchange in an emergent vegetation canopy (**) ***S. Huang, J. Yang***	Density currents interacting with an array of in-line and emergent cylinders ***A. Ricardo, G. Giampa, R. Ferreira, J. Ramos, M. Brito***
11:40	***Discussion Period***	**Discussion Period**	Experimental study of turbulent flow characteristics around a circular compound bridge pier ***S. Reddy, V. Chandra***	Flow resistance in open channels with leafed flexible vegetation and large-scale bedforms (**) ***G. Artini, S. Francalanci, L. Solari, J. Aberle***	An improvement to the particle tracking velocimetry algorithm applied to the study of a shallow mixing layer (**) ***J. Restrepo-Grisales, S. Gaskin***
12:00			Live bed scour depth modelling around bridge pier using Support Vector Machine (**) ***Nil, A. Baranwal, B. Das***	**Discussion Period**	**Discussion Period**
			12:20 Discussion Period		
12:15	Lunch Break, IAHR Fluvial Hydraulics Committee Meeting				

Tuesday – November 8th, Afternoon

13:15	Parallel Sessions 2				
	A3: Flow in Straight and Compound Channels – Part I ***Chair: Katinka Koll*** ***TU Braunschweig, Germany***	**B1: Sediment Transport – Part I** ***Chair: Joe Aberle*** ***TU Braunschweig, Germany***	**B2: Large-Scale River Morphodynamics – Part I** ***Chair: Volker Weibrecht*** ***ETH Zürich, Switzerland***	**D2: Ecological Aspects of River Flows – Part I** ***Chair: Giovanni De Cesare*** ***EPFL, Switzerland***	**F1: Extreme Events and Effects of Climate Change – Part I** ***Chair: Pierfranco Costabile*** ***University of Calabria, Italy***
13:20	A new perspective on turbulent boundary layer profiles ***G. Smart***	Evaluation of critical shear stress in channel beds of fine gravel (**) ***B. Oviedo Lorío, R. Murillo-Muñoz***	Saturation of curvature-induced secondary currents in relatively sharp bends: a two-dimensional modelling approach (**) ***T. Lazzarin, D. Viero***	Flume study on hydro-morphologic changes provided by instream tree installations **I. Schnauder, K. Blanckaert**	The value of globally available data for flow predictions in small catchments: a case study of the Aa of Weerijs, The Netherlands ***L. Umutoni, A. Jonoski, I. Popescu***
13:40	An iterative method for estimating the velocity dip positions across a river ***A. Handique, A. Sarma, R. Bhattacharjya***	Modelling bedload particle travel lengths in rivers with different hydrologic regimes (**) ***E. Papangelakis, B. MacVicar, A. Montakhab, P. Ashmore***	Application of convective flow model to a real meandering bend (**) ***H. Zhang, W. Dai***	Fish trajectories over a full-scale model of a nature-like unstructured block ramp (**) ***R. Eikenberg, J. Aberle, P. Andreasson, D. Aldvén, L. Persson***	Changes in the flow processes in the rivers of the Mura-Drava-Danube transboundary biosphere reserve ***E. Tamás, L. Tadić***
14:00	Comparing shallow mixing layers over rough and smooth beds (**) ***B. Cerino, S. Proust, C. Berni, V. Nikora***	Spatial and temporal variations of suspended sediment concentrations from different floodplain environments (**) ***C. Salas, B. Rhoads***	Simulation of potential meandering belt width using a physics-based morphodynamic model ***H. Amini, F. Monegaglia, M. Redolfi, M. Tubino, G. Zolezzi, S. Lanzoni***	Predicting spawning habitat distribution of P. altivelisin in gravel-bed rivers by computational model ***M. Harada***	Threshold identification using daily streamflow records for two stations along the Niger River, West Africa ***A. Olusola, S. Ogunjo, S. Adelabu***
14:20	Investigation of turbulence characteristics and mixing layer thickness in gravel bed flows ***D. Termini, F. Lavignani, N. Benistati***	Estimation of suspended-sediment rating curves in the Ca River Basin, Vietnam (**) ***C. Pham Van, H. Le, D. Nguyen-Ngoc***	Restoration of channel meandering using current deflectors (**) ***Y. Pi, C. Wu, Y. Cho, C. Zhang***	Linear theory for the formation of aquatic vegetation patches in rivers ***C. Carbonari, G. Calvani, L. Solari***	High-resolution topographical data and high-performance-computing tools for the morphodynamical modelling of realistic flood events ***S. Martínez-Aranda, D. Vericat, R. Batalla, P. García-Navarro***
14:40	Free surface flow past a single bar in a gravel stream and related hyporheic flow (**) ***M. Ahadi, A.M. Ferreira da Silva, A. Button***	Fluvial erosion of cohesive glacial sediments: clays and tills from the Great Lakes and St. Lawrence Lowlands (**) ***L. Gonthier, D. Yeats, S. Gaskin***	Meandering rivers in the midwestern US that anabranch: prevalence, morphological characteristics and power regimes (**) ***T. Shukla, B. Rhoads***	Developing a new conservation management tool: the Mussel Biosensor ***E. Curley, R. Thomas, C. Adams, A. Stephen***	GPU simulation of flood and erosion risk mitigation strategies in olive-grove basins ***P. Bohorquez, F. Pérez-Latorre, I. González-Planet, R. Jiménez-Melero, G. Parra***
15:00	**Discussion Period**	**Discussion Period**	**Discussion Period**	**Discussion Period**	**Discussion Period**
15:15	Afternoon Break				
15:30	Lab Visits: Universities of Waterloo, McGill and Ottawa				
16:00	Greet and Meet Session (REMO)				

Wednesday – November 9th, Morning

08:15	**Keynote Lecture 2** **Channel bed incision in engineered rivers: characteristics and mitigation** ***Dr. Astrid Blom, Professor, TU Delft, The Netherlands***				
09:15	Morning Break				
09:45	Parallel Sessions 3				
	B3: Innovative Measurement Techniques ***Chair: Patrick Grover*** ***BGC Engineering, Canada***	**B4: Sediment Transport – Part II** ***Chair: Rui Ferreira*** ***IST, Portugal***	**B5: Bifurcations and Confluences** ***Chair: George Constantinescu*** ***University of Iowa, USA***	**C2: In-Stream Structures: Hydrodynamics, Scour and Riverbed Protection – Part II** ***Chair: Wim Uijttewaal*** ***TU Delft, The Netherlands***	**F2: Extreme Events and Effects of Climate Change – Part II** ***Chair: Susanna Dazzi*** ***University of Parma, Italy***
9:50	Robust and accurate river flow measurement by Space-Time Image Velocimetry (STIV) with Improved Deep Learning Technique ***K. Watanabe, Y. Minami, M. Iguchi, I. Fujita***	Transport-supply ratios in river channels ***J. Haschenburger***	Flow partitioning at a bifurcation in the Upper Dutch Rhine (**) ***M. Chowdhury, A. Blom, R. Schielen***	Roll waves on a laminar sheet flow produced by local disturbance ***B. Yu, V. Chu***	Automatic calibration of a river reach in northern Italy by coupling a parallel 2D shallow water model and the PEST tool ***A. Ferrari, M. D'Oria, R. Vacondio, P. Mignosa***
10:10	Detection of morphological changes for Wadi channel bed in the arid region using SFM Photogrammetry (**) ***M. Al mamari, S. Kantoush, T. Sumi, M. Saber***	Living-Lab Rhine (LiLaR) – comparing Dutch and German sediment measurements in the border Rhine ***M. Struck, N. Huber, G. Hillebrand, P. Onjira, A. Winterscheid, J. Brils, R. Schielen, J. Mol, C. Bode, A. van den Hoek, F. Siering***	3D CFD modeling of bed changes at a laboratory channel confluence ***B. Balouchi, A. Mirzaahmadi, H. Bihs, N. Ruther***	An experimental study on scour beneath pipelines at river crossings ***M. Ahadi, A.M. Ferreira da Silva, P. Grover, K. Lockwood***	Lag time predictions using characteristic times deduced by the 2D Shallow Water Equations at basin-scale (**) ***K. Négyesi, E. D. Nagy, G. Barbero, G. Petaccia, C. Costanzo, P. Costabile***
10:30	Photogrammetry measurements of wave overtopping erosion on a seashore dike (**) ***M. Ebrahimi, M. Van Damme, S. Soares-Frazão***	Sediment balance for the supply-limited Meuse River ***H. Barneveld, T. Hoitink, R. Frings***	Observations and modeling of density-driven streamwise orientated vortices at a river confluence ***J. Duguay, P. Biron, J. Lacey***	Investigation of vorticity and coherent turbulent structure in a 90° lateral water diversion with and without a vane-field ***J. Baltazar, G. Bombar, E. Alves, A. Cardoso***	Influence of EURO-CORDEX ensemble on lumped flood impact indicators: a case study ***R. Padulano, G. Rianna, P. Mercogliano, P. Costabile, C. Costanzo, G. Del Giudice***
10:50	Retrieving channel geometry and flow properties of the Nicolet River from Satellite Multispectral Imagery ***B. Lak, S. Li***	Limits between surface and inner clogging of riverbed by fine sediment (**) ***R. Dubuis, G. De Cesare***	Bed morphology characterization of an anabranching bifurcation-confluence of the Solimões River, Brazil ***R. Gutierrez, F. Escusa, R. Almeida, M. Ianniruberto, C. Gualtieri***	Stability of consecutive stacked boulders behind Check Dams during flood stages ***N. Fuchino, Y. Yasuda***	Response of the Lower Rhine River to climate change over the period 2010-2050 (**) ***C. Ylla Arbós, A. Blom, R. Schielen***
11:10	**Discussion Period**	Experimental characterization of dry granular flows through sudden constrictions (**) ***S. Mendes, R. Farias, R. Aleixo, M. Larcher, T. Viseu, R. Ferreira***	Laboratory study of density-driven streamwise orientated vortices at a symmetric confluence ***J. Duguay, P. Biron, J. Lacey, C. Bergeron***	Impact of mud flow instabilities on hydraulic structures (**) ***B. Yu, V. Chu***	Flood hazard mapping in river mouths: the effect of river bar formation and the phase lag between tides and river discharge ***A. Ruiz-Reina, C. Zarzuelo, A. López-Ruiz***
11:30		**Discussion Period**	**Discussion Period**	**Discussion Period**	**Discussion Period**
11:45	Lunch Break				

Wednesday – November 9th, Afternoon

12:30	Video Clip Contest			
13:15	**Parallel Sessions 4**			
	A4: Physics and Modeling of Streamflows ***Chair: Samuel Li*** ***Concordia University, Canada***	**B6: Bed Forms** ***Chair: Gökçen Bombar*** ***Izmir Katip Çelebi University, Turkey***	**C3: Dams and Rivers: Sedimentation, Regulation, Restoration and Removal** ***Chair: Jason Duguay*** ***Concordia University***	**D3: Ecological Aspects of River Flows – Part II** ***Chair: Walter Bertoldi*** ***University of Trento, Italy***
13:20	Application of the extended Bernoulli equation to a potential flow in a rectangular contracted flume ***U. Teschke, F. Ruhr***	Dune bed statistical analysis using multibeam echosound survey data ***I. Cavalieri, L. Schippa***	Numerical modelling of navigable rivers: influence of navigation structures on the Meuse River flow ***A. Patil, J. Lambrechts, I. Draoui, F. Fiengo Perez, E. Deleersnijder***	Thermal responsiveness of small streams in frigid winters ***R. Ettema, E. Kempema***
13:40	The velocity of long wave in a channel of parabolic cross-section ***S. Sokolov***	Bedform morphology changes due to plastic pollution: preliminary observations and potential implications ***C. Russell, R. Fernández, D. Parsons, S. Gabbott***	Scale model study of simple energy dissipation features at low head dams ***M. Provan, P. Knox, A. Rayner, A. Cornett***	Quantification of environmental DNA transport over a river network ***L. Stancanelli, E. Ragno***
14:00	Mesh-free particle methods for simulation of fluvial processes, challenges and opportunities ***A. Shakibaeinia, M. Jandaghian***	Free alternate bars in a German sand bed river (**) ***T. Branss, J. Aberle, B. Hentschel***	Assessment of hydrological alteration in regulated water resources systems: a case study in the Júcar River basin (Spain) ***S. Ghannem, R. Bergillos, J. Paredes-Arquiola, A. Solera, J. Andreu***	Hydraulic attraction at a downstream bypass for European eels (**) ***S. Collier, R. Thomas, R. Wright, L. Carter, J. Bolland***
14:20	The discontinuous Galerkin method for river-delta continuum by means of a coupled 1D-2D shallow water model ***I. Draoui, J. Lambrechts, V. Legat, E. Deleersnijder***	Formation of repeating bedforms (bars-flats) in ephemeral channels: from field observations to modelling (**) ***G. Massera, A. Siviglia, M. Tubino, T. Cohen, J. Laronne, M. Dorman, I. Reid, D. Powell***	Numerical modelling investigation of low-water level events at a water intake near the Fort Frances-International Falls Dam **A. *Pilechi, E. Murphy***	Individual and collective plants motion in a submerged, staggered, flexible, artificial canopy ***L. Guiot, D. Doppler, J. Jerome, B. Löhrer. J. Frölich, N. Riviere***
14:40	Experimental and numerical investigation of the flow-structure of river surf waves ***P. Asiaban, C. Rennie, N. Egsgard***	Comparison of sand-bed river flow resistance calculations ***D. Froehlich***	Numerical modelling to estimate the reservoir sedimentation due to the implementation of Chepete dam in Beni River, Bolivia ***M. Jimenez, M. Heredia***	Experimental analysis on the stability of alternative gravel dikes during flood stages in channelized rivers (**) ***P. Beretta Piccoli, Y. Yasuda***
15:00	**Discussion Period**	**Discussion Period**	Managing negative values in reservoir inflow computation- a case study ***A. Shibu, S. Mukherjee***	Butterfly effect in a deterministic ecomorphodynamic model (**) ***I. Cunico, W. Bertoldi, A. Siviglia, F. Caponi***
			15:20 Discussion Period	**15:20 Discussion Period**
15:15	Afternoon Break			
15:45	Lab Visits: Universities of Sherbrooke and Queen's			
16:15	Social Hour (REMO)			

Thursday – November 10th, Morning

08:15	**Keynote Lecture 3** **What braiding reveals about river morphology, bedload and channel change** ***Dr. Peter Ashmore, Professor, University of Western Ontario, Canada***				
09:15	Morning Break				
09:45	Parallel Sessions 5				
	B7: Morphological Response to Human Activities ***Chair: Ronald Guierrez*** ***Pontifical Catholic Univ., Peru***	**B8: Bank Erosion and Protection** ***Chair: Pascale Biron*** ***Concordia University, Canada***	**D4: Stream Restoration and Conservation** ***Chair: Elli Papangelakis*** ***McMaster University, Canada***	**E2: Contaminant Transport and Mixing Processes – Part II** ***Chair: Mário Franca*** ***KIT, Germany***	**F3: Extreme Events and Effects of Climate Change – Part III** ***Chair: Michael Nones*** **Polish Acad. Sciences, Poland**
09:50	The effect of land use changes on the morphology of a small rural stream in southwestern Ontario, Canada ***S. Gardner, D. Nguyen, N. Sattolo, H. May, A. Binns, J. Levison***	Mechanistic 2D flow-erosion modelling of vegetated river banks **P. Perona, G. De Cesare, M. Schwarz**	Classification of mountain streams using Rosgen and Montgomery-Buffington methods (Case Study - Jajroud basin) ***M. Pirestani, A. Gashtasebi***	Sediment and chemical transport modeling of a hypothetical tailings dam breach spill in the lower Athabasca River (**) ***M. Taherparvar, A. Shakibaeinia, Y. Dibike***	How fast is “flashy”? Hydraulics of flood hydrographs in small urban rivers (**) ***A. Montakhab, B. MacVicar***
10:10	Predicting response of channel width along an urbanizing river channel ***V. Barlow, P. Ashmore, B. MacVicar***	Ship wave induced excess pore water pressure in riverbeds and banks - an investigation on silty sands ***J. Rothschink, O. Stelzer***	Designing channel corridors to improve hydroecological conditions in suburban streams ***J. Franssen, P. Villard***	Predicting sediment and heavy metal transport within the Lower Athabasca River using 1D numerical modelling ***S. Kashyap, A. Petty, C. Leidl, S. Depoe***	Understanding the impacts of hydraulic uncertainties on urban flood mapping (**) ***S. Abedin, B. MacVicar***
10:30	Evaluation of the impact of the Peruvian Waterway dredged channel in the bed morphodynamics of the Huallaga River ***H. Valverde, L. Guerrero, C. Frías, J. Abad***	Experimental characterization of root-reinforced riparian sediment deposits in a restored and widened river course ***G. De Cesare, M. Solioz, P. Perona***	Towards guidance on effective use of nature-based approaches to flood and erosion risk management in Canadian river basins ***I. Vouk, S. Ferguson, E. Murphy, A. Pilechi, M. Provan***	Water pollution during floods: a protocol for measuring concentration and calculating mass discharge across a straight street (**) ***C. Fagour, S. Proust, E. Mignot***	Numerical solution of Saint-Venant equations in flood wave prediction in the lower Tapi River, India ***S. Sahoo, K. Devi, J. Khuntia, K. Khatua***
10:50	Modelling the impact of sand extraction from large rivers ***A. Gasparotto, A. Nicholas, G. Sambrook Smith, A. Daham***	Geometric floodplain controls on riverbed elevation change within and between flood events (**) ***S. Ahrendt, A. Blom, R. van Denderen, R. Schielen, A. Horner-Devine***	Providing greater variability, degrees of freedom, retention and detention for resilience in restored stream corridors ***P. Villard, J. Franssen***	Different approaches for particle representation in plastic debris transport models ***C. Yan Toe, W. Uijttewaal, D. Wüthrich***	The impact of flood waves on hydraulic structures ***B. Yu, V. Chu***
11:10	Continuous monitoring of morphological changes from sediment augmentation by field measurements and flume experiments (**) ***C. Mörtl, G. De Cesare***	Bedform observations at the operative stage of a groyne system in the Madre de Dios River, Peru ***R. Gutierrez, F. Escusa, F. Núñez-Gonzáles, J. Moris, J. Jamanca***	Fulfilling Riverscape - a creative interdisciplinary approach ***T. Arborino, S. Nguyen, G. De Cesare, P. Perona***	An innovative point location method for particle tracking models with application to water quality modeling in rivers and coastal waters ***R. Boukhelif, A. Pilechi, S. Douglas***	Regional-scale 2D hydraulic modelling for the assessment of the residual flood hazard due to levee breaches ***S. Dazzi, P. Mignosa, M. Pianforini, R. Vacondio***
11:30	**Discussion Period**	**Discussion Period**	**Discussion Period**	**Discussion Period**	**Discussion Period**
11:45	Lunch Break				

Thursday – November 10th, Afternoon				
13:00	Parallel Sessions 6			
	B9: Large-Scale River Morphodynamics – Part II ***Chair: Jorge Abad*** ***RED YAKU, Peru***	**B10: Debris and Dam-Break Flows** ***Chair: Sandra Soares-Frazão*** ***U. Cath. Louvain-la-Neuve, Belgium***	**C4: In-Stream Structures: Hydrodynamics, Scour and Riverbed Protection – Part III** ***Chair: Emmanuel Mignot*** ***INSA-LYON, France***	**D5: Large Wood in Rivers and Streams** ***Chair: Virginia Ruiz-Villanueva*** ***University of Lausanne, Switzerland***
13:05	A multi-scale braided river substrate map – case study in the Rangitata ***J. Rogers, J. Brasington, J. Hoyle, J. Tonkin***	Application of the SPH-Method to simulate debris flow in a torrent in Switzerland ***R. Züger, D. Farshi***	Superposition principle for the stage discharge relationships of complex weirs ***I. Bechoua, N. Rivière, Y. Peltier, E. Mignot***	Empirical prediction of large wood transport during flood events ***N. Steeb, A. Badoux, C. Rickli, D. Rickenmann***
13:25	Coevolution of morphology, flow conditions and pulsed transport in a laboratory-scale braided river: numerical simulations ***J. Tunnicliffe, P. Ashmore***	Numerical simulation of debris flows occurred in Marumori in 2019 and countermeasures against debris flow using the numerical simulation result ***H. Takebayashi, M. Fujita***	Similarity in longitudinal decays of free jump and submerged hydraulic jump ***S. Choi, S. Choi***	Variation of large wood load in a river affected by a volcanic eruption ***A. Iroumé, K. Sanchez, N. Ampuero, L. Picco***
13:45	Are we measuring morphological changes in gravel bed rivers with the appropriate frequency? ***E. Pandrin, W. Bertoldi***	Experimental study on the breach of landslide dams with different material compositions ***J. Yang, Z. Shi, S. Soares-Frazão, H. Zheng, D. Shen***	Riverbed protection due to consecutive stacked boulders at downstream of apron in movable weir ***S. Suzuki, Y. Yasuda***	Detecting instream wood transport by a custom Neural Network and Radio Frequency Identification (RFID) technology ***J. Aarnink, M. Vuaridel, V. Ruiz-Villanueva***
14:05	Dynamic river widening under variable bed-load supply ***C. Rachelly, D. Vetsch, R. Boes, V. Weibrecht***	Frozen in time: continuous measurements in a dam breach flow ***T. Alvarez, R. Aleixo, S. Mendes, S. Amaral, T. Viseu, R. Ferreira***	Fully Lagrangian mesh-free modelling of river ice interaction with control structures ***C. Billy, A. Shakibaeinia,T. Ghobrial***	Dynamics of submerged large wood debris in reservoirs and their potential risks to hydraulic structures ***S. Takata, T. Koshiba, T. Sumi***
14:25	Long-term reach-scale suspended sediment budget of a small creek with cohesive banks ***N. Al-Ghorani, M. Hassan, E. Langendoen***	Overtopping failure of a homogeneous earth-fill dam with two different breach sizes and rough downstream conditions ***E. Taşkaya, Z. Büyüker, B. Öztürk, G. Bombar, G. Tayfur***	Three-dimensional numerical modeling of a vertical slot fish pass with complex roughness distribution ***F. Scolari, S. Schwindt, S. Haun, S. Wieprecht***	Will woody debris accumulation alter the self-cleaning ability of a piano key weir? ***M. Panthi, B. Crookston***
14:45	**Discussion Period**	**Discussion Period**	**Discussion Period**	**Discussion Period**
15:00	Break			
15:15	Closing Ceremony			

Flow structure in a compound channel: benchmarking 2D and 3D numerical models

I. Kimura
University of Toyama, Toyama, Japan

D. Bousmar
Service Public de Wallonie, Châtelet, Belgium

P. Archambeau, B. Dewals, S. Erpicum, M. Pirotton, & X. Li
University of Liege, Liege, Belgium

D. Đorđević, N. Rosić & B. Zindović
University of Belgrade, Belgrade, Serbia

I. Echeverribar, A. Navas Montilla, P. Brufau & M.P. García Navarro
University of Zaragoza, Spain

M. Gonzales de Linares
Artelia, Echirolles, France

A. Paquier
Inrae Riverly, Villeurbanne, France

R. Kopmann
Federal Waterways Engineering and Research Institute, Karlsruhe, Germany

ABSTRACT: The benchmarking test of 2D and 3D numerical models on a compound channel flow with a rectangular shaped main channel and a rectangular shaped floodplain was carried out by the IAHR Working Group on Compound Channels. The selected test case is the flume experiment by Nezu and Tominaga (1991). Nine depth-averaged 2D models and four 3D models participated in the benchmark. In the 2D models, the depth averaged streamwise velocity profiles in the lateral direction were compared. In the 3D models, velocity components in three directions as well as the distribution of the turbulence kinetic energy in a cross-section were compared. Through the comparison, the applicability and limitations of each model are highlighted and discussed with regard to the model characteristics.

1 INTRODUCTION

Rivers with a compound cross-sectional shape have specific features in terms of stability of the flow path and effective use of the floodplain. With increasing discharges, the floodplain is overflowed and the structure of the flow becomes more complex. At the interface between floodplain and main channel, unsteady flow due to shear instability occurs. The secondary current of the Prandtl's second kind caused by the an-isotropy of turbulence in a cross section (Prandtl, 1931) is affected by the oblique ascending flow from the corner at the interface. Therefore, clarification and modelling of a compound channel flow is still a challenging topic in fluvial engineering.

Numerical analysis is one of the promising options for elucidating such a complex flow. A wide variety of numerical models are used in fluvial engineering field. There are one-dimensional models, two-dimensional depth averaged models, three-dimensional models, etc. as classification focuses on spatial dimensions; and RANS models, LES models etc. as classification focuses on turbulence models. Therefore, it is important to understand the characteristics of each model and then select a model that is suitable for the target and purpose. In the field of river engineering with relatively shallow water depths compared to the river widths, two-dimensional depth averaged models are typically applied and their high accuracy and economic efficiency have been shown in many cases. In cases of compound channel flows, it has also been shown that the depth averaged 2D model is applicable when the water depth is small compared to the width and/or when

the inclination angle of the main channel revetment is small (Bousmar et al. 2016). However, when the water depth is deep or when the cross-sectional shape of the main channel is rectangular, it is expected that the three-dimensionality of the flow will be remarkable. It is therefore important to examine the limits of the 2D depth averaged model and the applicability of the 3D model to such cases.

The IAHR Working Group on Compound Channels has been active since 2007 under the auspices of the Fluvial Hydraulic Committee. The objectives of this group are to foster collaboration and research on Compound Channel analysis and modelling. Setting up a benchmarking program is part of its activities. In this study, the benchmarking test covers a compound channel with a rectangular shaped main channel and a rectangular shaped floodplain. It focuses on the detailed modelling of the flow structures. The selected test case is the flume experiment by Nezu and Tominaga (1991). The aspect ratio of the cross-section of the main channel is $b/H = 2.5$ (b: width, H: depth in main channel, Figure 1), which is smaller than the ratio in natural rivers. Nine depth averaged 2D models and four 3D models from ten research institutions participated in the benchmark. In the 2D models, the depth averaged streamwise velocity profiles in the lateral direction were compared. In the 3D models, velocity profiles in x, y and z directions as well as the profile of the turbulence kinetic energy (TKE) in a cross-section were compared. Through the comparison, the applicability and limitations of each model are highlighted and discussed with regard to the model characteristics.

2 CONDITIONS FOR THE BENCHMARK TEST

2.1 *Outline of the reference data*

Experimental results by Tominaga & Nezu (1991) were used as reference data. The measurements were performed in a 12.5 m long 0.4 m wide channel. The bed wall and the sidewalls were composed of a painted iron plate and glass, respectively. The geometry of the cross-section of the channel is depicted in Figure 1. Both the main channel and the floodplain have rectangular shaped cross-sections. The experimental conditions and the discharges in each case are listed in Table 1. Four experiments cover different floodplain heights and roughness of the floodplain.

A two-dimensional fiber-optic laser doppler anemometer (FLDA) was used to measure velocities. The sampling frequency was 100 Hz and the sampling time was 50 sec. The error between both measured values of U was within about ± 1.5% of the maximum velocity, and the error of measured values of u' was within about ± 3% of the maximum turbulence intensity.

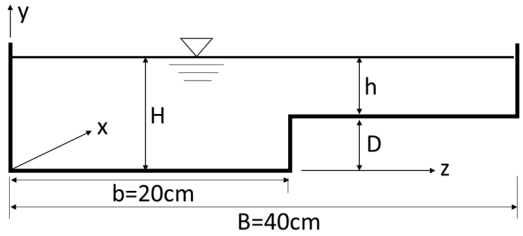

Figure 1. Geometry of the cross-section of the experimental flume

Table 1. Hydraulic conditions in the experiment

Case	H	h	Q	R_c	U_*	k_s	S_0
	cm	cm	ℓ /s	Cm	m/s	mm	
S1	8.03	6.03	10.3	5.02	0.0164	(Smooth bed)	0.000547
S2	8.00	4.00	8.38	4.29	0.0164	(Smooth bed)	0.000640
S3	8.05	2.05	5.82	3.60	0.0141	(Smooth bed)	0.000563
R1	8.05	4.05	6.70	4.31	0.0161	2	0.000613

Note: R_c: compound hydraulic radius, k_s: roughness height, S_0: estimated channel slope

The depth-averaged streamwise velocity profile along a cross-section in four cases are shown in Figure 2 together with the computed results. The characteristic is that the flow velocity drops near the interface between the main channel and the floodplain (z = 0.2m). It is thought that the

cause of this are effects of friction on the vertical wall of the main channel at the interface and oblique ascending current from the edge of the floodplain.

The contours of streamwise velocity in a cross-section in cases S2 and S3 are shown in Figure 3 together with the computed results. In all cases, the maximum velocity occurs at a point below the surface in the main channel. This phenomenon is called velocity-dip and it is caused by the secondary current. The cross-sectional velocity vectors in cases S2 and S3 are shown in Figure 4 with computed results. Secondary current of the second kind is observed in all cases. An inclined upflow from the corner of the interface, which is a typical characteristic in a compound channel flow, is also present in all cases. The profile of turbulence kinetic energy (TKE) in case S2 is shown in Figure 5. The maximum value of TKE is observed near the corner of the interface.

2.2 *Rules of the benchmark*

This benchmark was open for 2D and 3D numerical models. The flow can be assumed uniform in the streamwise direction. Therefore, the computed results are required at only one cross-section. In 2D models, participants should have provided the lateral distribution of the depth-averaged longitudinal velocity U at the measured points by Tominaga and Nezu (1991). In 3D models, the 3D velocity components (u, v, w) and TKE at each measured grid points (y, z) should have been provided. The test case was done in two steps:

- Step 1 (blind step): With the given setup and geometry, each participant used his model with 'generic' parameters. In this step, the experimental data were not provided.
- Step 2 (tuning step): The results were compared to the measured data, and each participant could have 'tuned' his model parameters to improve the results.

After the two steps, the performances of all models were compared and examined.

3 RESULTS AND DISCUSSION ON 2D MODELS

3.1 *Participating 2D models*

In 2D case, nine models participated in the benchmark. All models are based on the depth-averaged shallow water equations. Turbulence model, type of computational grid and additional remarks are listed in Table 2. In all models, RANS type turbulence model (0-equation or k-ε models) were used. As for computational grid, both rectangular and unstructured grid were used.

Table 2. Participating 2D models

Model	Model name	Turbulence model	Grid	Boundary conditions	Remarks	References
2D-a	RiverFlow2D	no turbulence diffusion	Adaptive triangular		FVM	Murillo et al. (2007) Murillo et al. (2008)
2D-b	SW WA	depth average mixing length model	Structured quadrilateral	No-periodic B.C.	High resolution FVM, Roe Riemann solver	Navas-Montilla et al. (2019)
2D-c	PEKA2D	No turbulence diffusion	Unstructured triangular	No-periodic B.C.	FVM, 1st order Roe-type Riemann solver with wall	Echeverribar et al. (2019)
2D-d	Ibar	Mixing length model	Unstructured quadrilateral	No-periodic B.C.	FVM, high resolution upwind scheme of Roe	Bladé et al. (2014), Cea et al. (2015), Cea et al. (2007)
2D-e	Rubar 20	constant eddy viscosity coef. ν_t= 0.00001m^2/s	Rectangular	No-periodic B.C.	FVM explicit and 2nd-order accurate	Bazin et al. (2017), Mignot et al. (2006)
2D-f	Telemac 2D	Standard k-ε	Unstructured triangular	No-periodic B.C.	FEM, Lateral wall friction computed assuming a hydraulically smooth flow	Galland et al. (1991) Hervouet (2007) Telemac-Mascaret (2022)
2D-g	iRIC, Nays2DH	Standard k-ε	Rectangular	Periodic B.C. No sidewall resistance	FVM	Iwasaki et al. (2016)
2D-h	WOLF	Two-length-scale depth-averaged k-ε model	Cartesian	No-periodic B.C.	FVM. Diffusion is computed using the specific discharge and not the velocity.	Camnasio et al. (2014), Dufresne et al. (2011), Erpicum et al. (2009), Erpicum et al. (2010)
2D-i	WOLF-OO	Two-length-scale depth-averaged k-ε model (alternate implementation)	Cartesian	No-periodic B.C. No sidewall resistance	FVM	-

3.2 *Results of 2D models*

Figures 2 (a)-(d) compare the depth-averaged streamwise velocity (U) profiles in a transverse direction computed by the nine models to the experimental data. The calculation results differ enormously depending on the model. In this benchmark, the ratio between the main channel width and the depth is smaller than that in a typical river. Therefore, the velocity profile is significantly affected by the three-dimensional flow structure characterized by the secondary current of the second kind. It is obvious that there is a limitation to the applicability of 2D models. It is necessary to keep this limitation in mind when discussing the results.

Generally, the computed velocities in the main channel are larger than those in the experiment. This could be due to the development of 3D flow structures. The present geometries have low width to depth ratio for the main channel. Another explanation, not to be excluded, is a flaw in the experimental data, with a too large discharge introduced on the floodplain at the inlet section. All simulations are expected to be done with the same flow depth. Integration of the velocity profile should give the same discharge. It appears that some simulations give lower cross-sectional averaged velocity. A possible explanation is the setting of boundary conditions. Periodic boundary conditions guarantee proper flow depth, but not proper discharge. Fixing downstream level and upstream discharge guarantee proper discharge, but not flow depth.

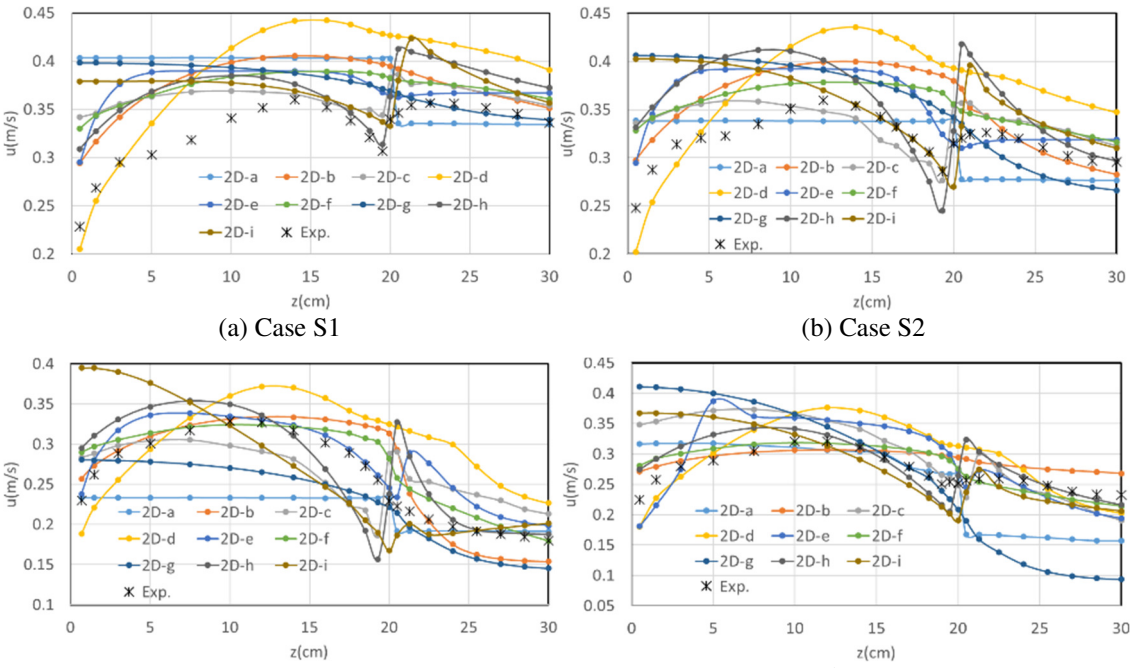

(a) Case S1 (b) Case S2

(c) Case S3 (d) Case R1

Figure 2. Comparison of computed depth-averaged streamwise velocity profiles in a cross section.

3.3 *Discussion of results with 2D models*

3.3.1 *Effect of turbulence model*

Turbulence diffusion terms are included in most of the models except models 2D-a and 2D-c. In those models, turbulence from the bed is considered only in the bed friction term. In the result of model 2D-a, the velocities in the main channel and on the floodplain are almost uniform due to the lack of lateral momentum diffusion. However, model 2D-c, which also does not include the diffusion term, surprisingly shows a curved velocity profile. The reason is that the model 2D-c uses an unstructured grid while model 2D-a uses adaptive triangular grid. The unstructured mesh in 2D-c is not aligned with the bank crest. This generates mixing and artificial diffusion.

3.3.2 *Sidewall friction*

In the experimental results, the velocity decreases near the sidewall of the main channel. One of the causes of this velocity deceleration is a wall friction. In addition, the secondary current also affects the depth-averaged velocity decrease near the sidewall of the main channel. On the other

hand, according to the experimental results, the velocity is not so affected by the sidewall on the floodplain. The reason is that the influence of the sidewall on the velocity is relatively small compared to the influence of bottom friction because the depth is smaller than the depth in the main channel. The models 2D-a, 2D-g and 2D-i did not consider the sidewall friction. Figure 2 shows a clear difference between the results of the models with and without sidewall resistance.

3.3.3 *Velocity profile near the interface*

Modelling of the vertical main channel bank at the interface is a challenging task. In all participating models, steep slope on one or a few cell widths approximates interfacial vertical wall. As shown in Fig. 2, experimental results except for the case S3 show a velocity dip at the interface between the main channel and the floodplain. Only models 2D-h and 2D-i seemed to reproduce this velocity dip while other models failed to capture it. On the other hand, these two models also overpredicted the velocity on the floodplain near the interface. This behaviour is caused by the different expression of turbulent diffusion terms. In the depth-averaged model, the momentum equation in x-direction is

$$\frac{\partial hU}{\partial t}+\frac{\partial hUU}{\partial x}+\frac{\partial hUW}{\partial z}+gh\frac{\partial h}{\partial x}=gh\sin\theta-\frac{\tau_{bx}}{\rho}+\frac{\partial}{\partial x}\left(h\nu_t\frac{\partial U}{\partial x}\right)+\frac{\partial}{\partial z}\left(h\nu_t\frac{\partial U}{\partial z}\right) \quad (1)$$

where U and W are the components of depth-averaged velocity vector in x and z directions, respectively, h: depth, g: gravity acceleration, τ_{bx}: bed shear stress in x-direction, θ: bed slope angle and ν_t: the eddy viscosity coefficient. The diffusion term in the lateral direction (the fourth term in the right-hand side of the equation (1)) determine the cross-sectional velocity profile. In 2D-h and 2D-i, the diffusion terms are expressed in a little bit different way as a function of the specific discharge, and is modelled as

$$\frac{\partial}{\partial x}\left(\nu_t\frac{\partial hU}{\partial x}\right)+\frac{\partial}{\partial z}\left(\nu_t\frac{\partial hU}{\partial z}\right) \quad (2)$$

The fourth term in (1) has an effect to smooth the depth-averaged velocity U in the lateral direction, while the second term in (2) flattens the profile of flux hU. If there is a gap in the depth, like that at the interface, the velocity U also changes suddenly in the opposite direction to homogenize the flux across the gap. That is the reason why models 2D-h and 2D-i seemed to capture the velocity lowering around the interface, although it is unsure whether the actual physical process is captured as it is intrinsically 3D.

3.3.4 *Quantitative evaluation of model accuracy*

For objective and repeatable comparison of different models, percentage error E is computed for each value:

$$E=\frac{V_{comp}-V_{meas}}{V_{meas}} \quad (3)$$

where V_{comp} = computed value; and V_{meas} = measured value.

The errors were aggregated as mean percentage error *MPE* and root mean square error *RMSE:*

$$MPE=\frac{1}{n}\sum E=\frac{1}{n}\sum\frac{V_{comp}-V_{meas}}{V_{meas}},\ RMSE=\sqrt{\frac{1}{n}\sum E^2}=\sqrt{\frac{1}{n}\sum\left(\frac{V_{comp}-V_{meas}}{V_{meas}}\right)^2} \quad (4)$$

where n is the number of measurement points. In MPE, positive and negative errors are canceled and then it can measure the bias of the simulated results.

A global performance ranking was given for each data series, based on MPE and RMSE values. Notes were given from AAA for both *MPE* and *RMSE* < 2% to EEE for both values > 25 % using a matrix approach similar to Bousmar et al. (2016). For the present benchmark, MPE values for the four cases and nine models are in the range -12 to 18% and *RMSE* values are in the range 10 to 40%. Three models obtained a B ranking for one single case, but most results were ranked D to E. Moreover, one model obtaining a B ranking is model 2D-i for case R1, whose results were discussed in previous paragraph. The performance ranking based on the *MPE* and the *RMSE* was found less relevant than expected, based on the first benchmark experience.

Table 3. Participating 3D models.

Model	name	Turbulence model	Grid	B.C.	Scheme	References
3D-a	Ansys Fluent 14.0	Reynolds stress transport model	Structured rectangular	wall-law, Symmetric B.C. at surface, Periodic B.C. for inlet and outlet (length = 3m)	VOF	Ansys Fluent (2022)
3D-b	SSIIM2	Standard k-ε	Structured rectangular	Symmetric B.C. at surface wall-law, Non-periodic B.C. for inlet and outlet (length = 10m)	SIMPLE method 2nd order upwind rigid-lid model	Olsen (2000)
3D-c	iRIC, NaysCUBE	3rd order non-linear k-ε	Structured, Rectangular in horizontal and hexahedral in vertical	kinematic condition at surface Periodic B.C. for inlet and outlet, wall-law (length = 1m)	TVD-Muscl Adams-Bashforth in time	Kimura et al. (2001), Kimura et al. (2010)
3D-d	OpenFOAM	k-ω SST multiphase	Uniform on x axis, non-uniform on yz plane	Rough friction on all walls, Atmospheric pressure on top air boundary, Non-periodic B.C. for inlet and outlet (length = 12.5m)	VOF, 1st order in time (Euler), 2nd order on velocities	Menter et al. (2003)

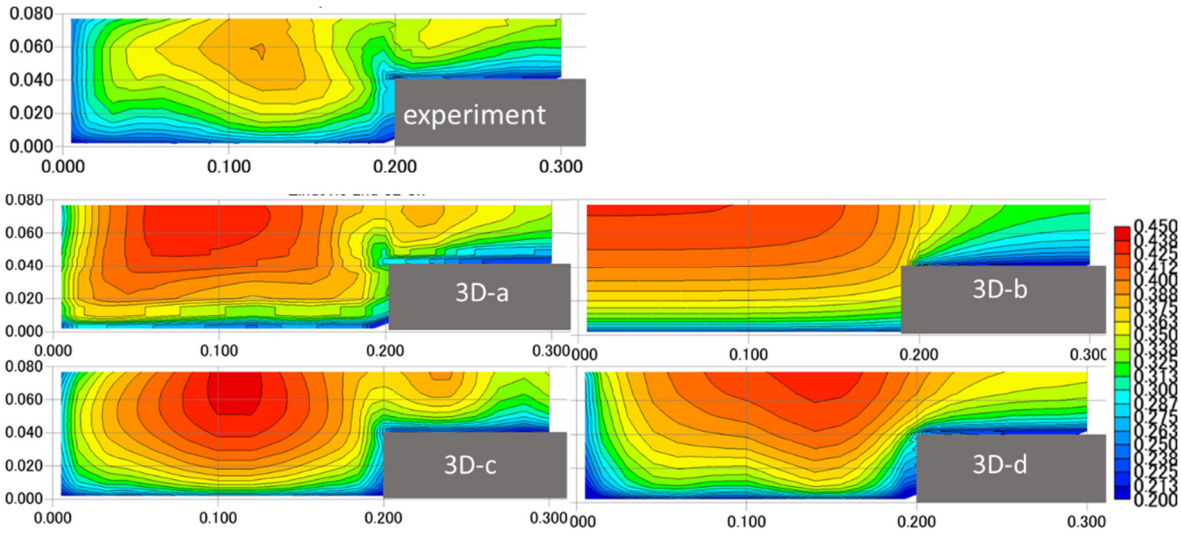

(a) case S2

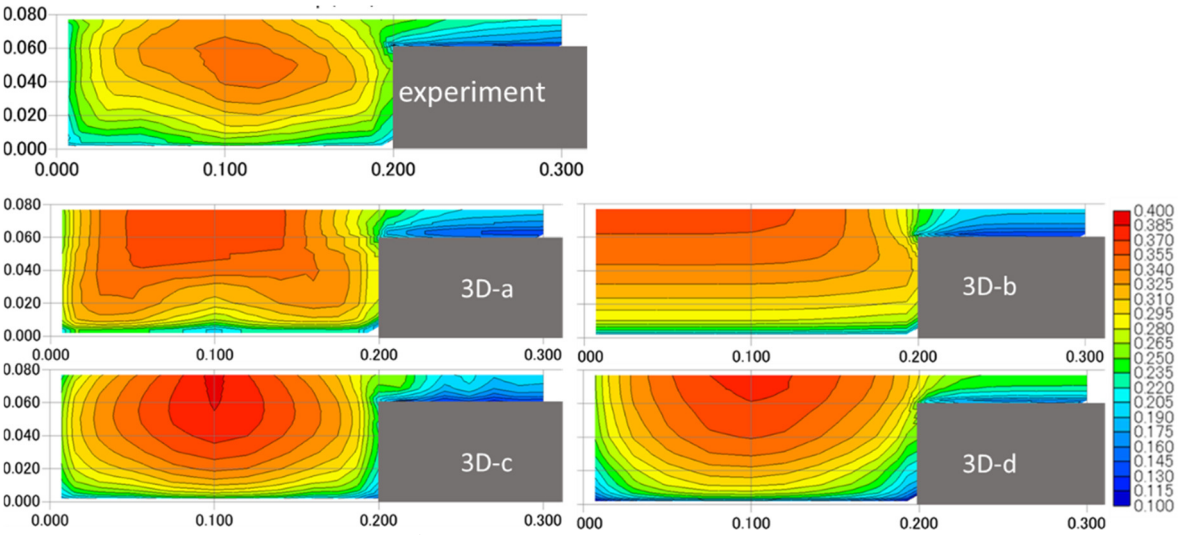

(b) case S3

Figure 3. Comparison of streamwise velocity contour in a cross section.

4 RESULTS AND DISCUSSION ON 3D MODELS

4.1 *Participating 3D models*

Four 3D models listed in Table 3 participated in the benchmark. In the present case, all models used structured rectangular mesh. Models 3D-a and 3D-c used periodic boundary conditions (enabling to model a much shorter flume than the actual one) and non-linear turbulence models, while 3D-b and 3D-d used standard boundary conditions and linear turbulence models.

4.2 *Results of 3D models*

Computed streamwise velocity (u) contours, velocity vectors (v, w) and TKE contours are shown in Figures 3, 4 and 5. Due to the space limitation, only the results in cases S2 and S3 are shown.

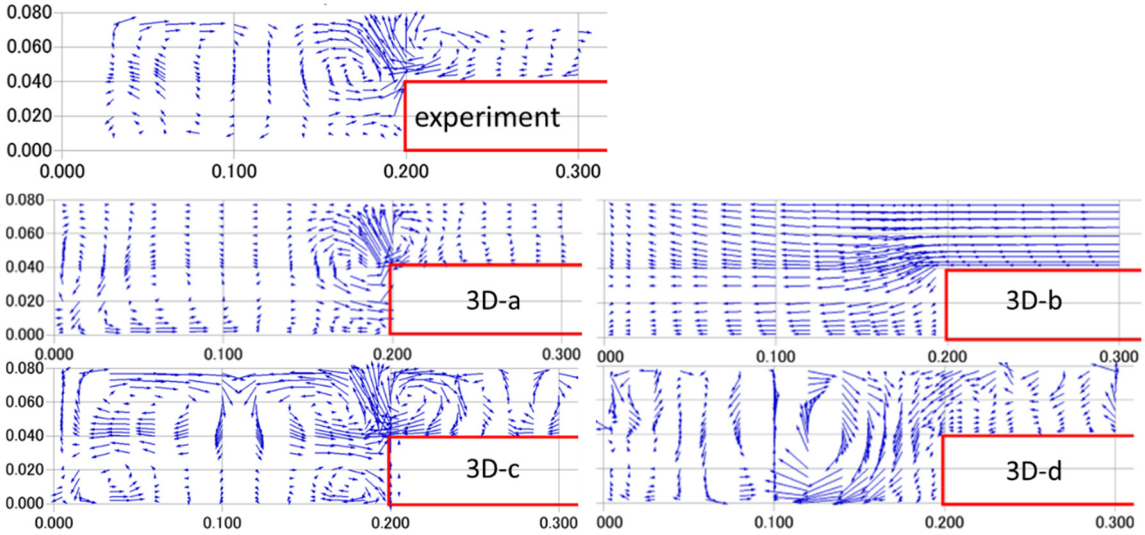

(a) case S2

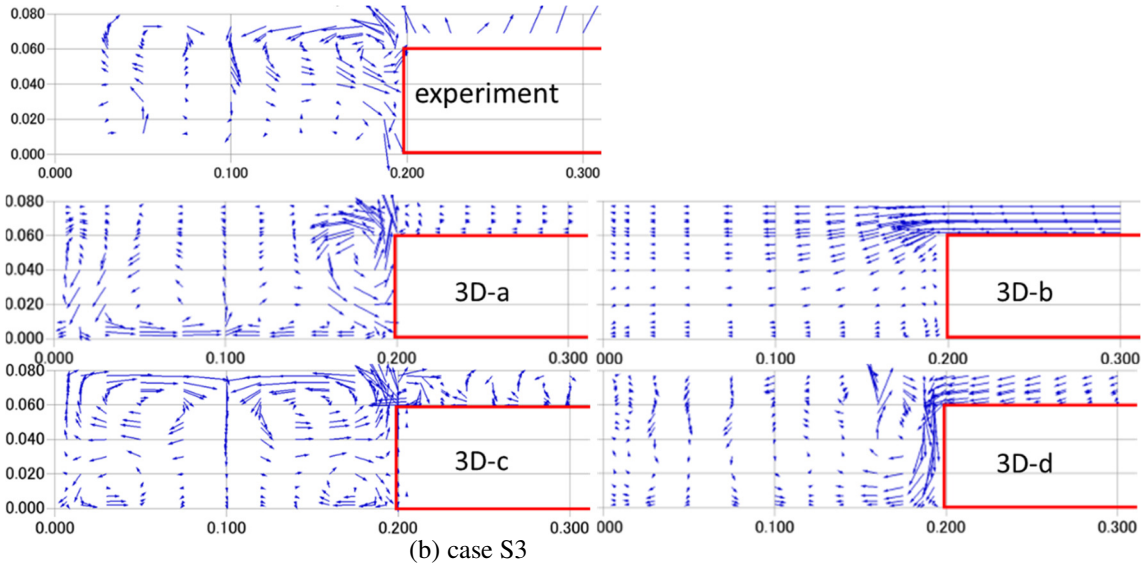

(b) case S3

Figure 4. Comparison of velocity vectors in a cross section.

4.3 *Discussion of results with 3D models*

4.3.1 *Effects of boundary conditions*

The choice of boundary conditions has a significant impact. Because the sidewall friction was neglected only in computation of 3D-b, the contour lines of velocity and TKE near the vertical

walls are unreasonably orthogonal to the sidewalls. Simulations 3D-b and d are done with classical upstream and downstream boundary conditions, while 3D-a and 3D-c employed the periodic boundary conditions. In the simulation of 3D-b, the computational domain was set shorter than in the experiment. It appears that the length is not enough to converge to equilibrated discharge distribution between subsections and that significant transverse velocities are still observed through the interface at the observation section (mid-length). In experiments, the maximum velocity in the main channel is found below the water surface, due to secondary currents. In all models, the maximum velocity is closer to the surface. This could be due to the free-surface modelling. In simulations 3D-a a multiphase model is used. Velocity of the air flow or symmetry hypothesis could impact the results. In simulations 3D-b, a rigid lid hypothesis is used, with a symmetrical velocity profile. In simulations 3D-c, kinematic boundary condition is imposed.

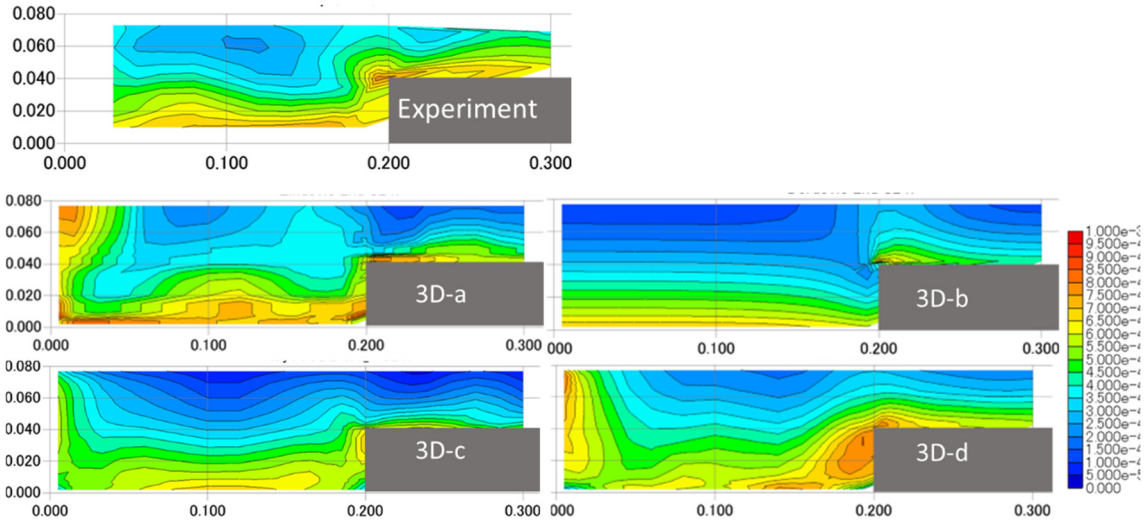

(a) case S2

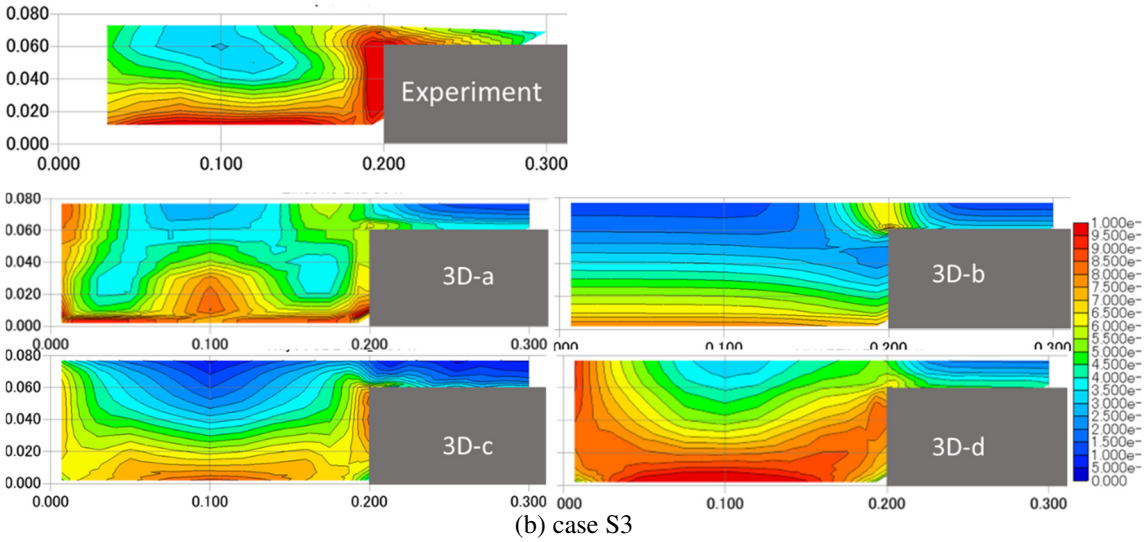

(b) case S3

Figure 5. Comparison of TKE contours in a cross section in case S2.

4.3.2 *Effects of turbulence model*

The choice of linear turbulence models (3D-b and 3D-d) or non-linear turbulence models (3D-a and 3D-c) influences the results. Secondary currents of the second kind were only reproduced with non-linear models. Even the results with a non-linear model did not manage to capture the actual flow shape precisely. Notably the upward flow at the interface corner is observed inclined toward the main channel but modelled vertical. The recirculation cell on the floodplain in 3D-d is inverted in case S2.

4.3.3 *Quantitative evaluation of models' accuracy*

The ranking of each model was also obtained in the similar way as for the 2D models (see 3.3.4). As a result, model 3D-d showed the highest score. However, the qualitative characteristics in the results of 3D-d are different from those of the experiment, such as the secondary cell near the interface being reproduced in the opposite direction to the experiment. This indicates that the ranking criteria may be inappropriate for evaluating 3D models.

5 CONCLUDING REMARKS

The IAHR Working Group on Compound Channels conducted a benchmarking for 2D and 3D computational models. The experimental data of Tominaga & Nezu (1991) was employed as the reference data. In this experiment, strong 3D flow structures were expected due to the relatively deep main channel as well as the vertical side and interfacial walls.

In 2D, the presence/absence of the turbulence model and the boundary conditions of the sidewall greatly affected the calculation accuracy. It was also shown that the modelling of the turbulent diffusion term has a great influence on the reproduction of the decrease in the flow velocity near the interface observed in the experimental results. On the other hand, for 3D models, the boundary conditions at the free surface are important for reproducing velocity-dip phenomena. As for the cross-sectional flow patterns, the boundary conditions between inlet and outlet and the choice of the turbulence model (linear or non-linear) were shown to be important. In addition, we tried ranking by *MPE* and *RMSE* to evaluate each model objectively and quantitatively. However, it was shown that such general metrics were not always appropriate for assessing the model performance under the present condition, because they lump many effects into a single number and they fail to point at specific features of the observed and computed flows. The same was observed in benchmarking exercises in other fields such as for streamflow models (de Boer-Euser et al., 2017).

ACKNOWLEDGEMENT

We would like to express our sincere gratitude to Professor Akihiro Tominaga for providing us with the experimental data.

REFERENCES

Ansys Fluent website. 2022. https://www.ansys.com/products/fluids/ansys-fluent

Bazin, P.H., Mignot, E., & Paquier, A. 2017. Computing flooding of crossroads with obstacles using a 2D numerical model. *Journal of Hydraulic Research*, 55(1):72-84.

Bladé, E., Cea,L., Corestein, G., Escolano, Puertas, J., Vázquez-Cendón, ME., Dolz, J. & Coll, A. 2014. Iber: herramienta de simulación numérica del flujo en ríos. *Revista 95 Internacional de Métodos Numéricos para Cálculo y Diseño en Ingeniería*, 30(1):1-10.

Bousmar, D. et al. 2016. Uniform flow in prismatic compound channel: benchmarking numerical models. *RiverFlow 2016*, Boca Raton: CRC Press.

Camnasio, E., Erpicum, S., Archambeau, P., Pirotton, M. & Dewals, B. 2014. Prediction of mean and turbulent kinetic energy in rectangular shallow reservoirs, *Eng. App. of Comp. Fluid Mech.*, 8(4):586–597.

Cea, L. & Bladé, E. 2015. A simple and efficient unstructured finite volume scheme for solving the shallow water equations in overland flow applications. *Water Resources Research*, 51(7):5464-5486.

Cea, L., Puertas, J. & Vázquez-Cendón, ME. 2007. Depth-averaged modelling of turbulent shallow water flow with wet-dry fronts. *Archives of Computational Methods in Engineering (ARCME)*, 14(3).

de Boer-Euser, T., Bouaziz, L., De Niel, J., Brauer, C., Dewals, B., Drogue, G., ... & Willems, P. (2017). Looking beyond general metrics for model comparison–lessons from an international model intercomparison study. *Hydrology and Earth System Sciences*, 21(1), 423-440.

Echeverribar, I., Morales-Hernández, M., Brufau, P. & García-Navarro, P. 2019. 2D numerical simulation of unsteady flows for large scale floods prediction in real time, *Advances in Water Resources*, 134:103444.

Erpicum, S., Meile, T., Dewals, B. J., Pirotton, M. & Schleiss, A. J. 2009. 2D numerical flow modeling in a macro-rough channel, *Int. J. for Numerical Methods in Fluids*, 61(11):1227-1246.

Erpicum, S., Dewals, B.J., Archambeau, P. & Pirotton, M. 2010. Dam break flow computation based on an efficient flux vector splitting, *J. of Comp. and App Math.*, 234(7):2143-2151.

Galland, J.C., Goutal, N. & Hervouet, J.M. 1991. TELEMAC: A New Numerical Model for Solving Shallow Water Equations. *Advances in Water Resources*, 14(3):138–148.

Hervouet, J.M. 2007. *Hydrodynamics of Free Surface Flows: Modelling with the finite element method*. DOI:10.1002/9780470319628. John Wiley & Sons, Ltd.

Iwasaki, T., Shimizu, Y. and Kimura, I. 2016. Numerical simulation of bar and bank erosion in a densely vegetated floodplain: A case study in the Otofuke River, *Advances in Water Resources*, http://dx.doi.org/10.1016/j.advwatres.2015.02.001.

Kimura, I., Takimoto, S., Blanckaert, K., Shimizu, Y. & Hosoda, T. 2010. 3D RANS computations of open channel flows with a sharp bend, *Environmental Hydr.*, Boca Raton: CRC Press, 961-966.

Kimura, T., Hosoda & T. Sakurai. 2001. Prediction of Flow Characteristics in Compound Open Channels by Means of a Non-linear k-ε Model, *3rd Int. Symp. on Envir. Hydr.*, Tempe, USA, 5-8.

Menter, F., Ferreira, J.C., Esch, T. Konno, B. & Germany, A.C. 2003. The sst turbulence model with improved wall treatment for heat transfer predictions in gas turbines. *Proc. the int. gas turbine congress*, 2–7.

Menter, F., Kuntz, M. & Langtry, R. 2003. Ten years of industrial experience with the SST turbulence model. *4th int. symp. on turbulence, heat and mass transfer*, 625–632, Antalya, Turkey.

Mignot, E., Paquier, A., Haider, S. 2006. Modeling floods in a dense urban area using 2D shallow water equations. *Journal of Hydrology*, 327(1-2):186-199.

Murillo, J., Burguete, J., Brufau, P. & García-Navarro, P. 2007. The influence of source terms on stability, accuracy and conservation in two-dimensional shallow flow simulation using triangular finite volumes. *International Journal of Numerical Methods in Fluids,* 54:543-590.

Murillo, J., Garcia-Navarro, P., & Burguete, J. 2008. Analysis of a second-order upwind method for the simulation of solute transport in 2D shallow water flow. *International Journal for Numerical Methods in Fluids*. 56(6):661-686.

Navas-Montilla, A., Juez, C., Franca, J.M. & Murillo, J. 2019. Depth-averaged unsteady RANS simulation of resonant shallow flows in lateral cavities using augmented WENO-ADER schemes. *Journal of Computational Physics*. 395:551-536.

Olsen, N.R.B. 2000. *CFD algorisms for hydraulic engineering*, PhD Thesis, Norwegian University of Science and Technology.

OpenFOAM website. 2022. https://www.openfoam.com/.

Prandtl, L. 1931. *Einführung in die Grundbegriffe der Strömungslehre* (Akademische Verlagsgesellschaft.

TELEMAC-MASCARET website. 2022. opentelemac.org.

Tominaga, A. & Nezu, I. 1991. Turbulent Structure in Compound Open-channel Flows. *Journal of Hydraulic Engineering, ASCE* 117(1): 21-41.